Available online at www.sciencedirect.com
ScienceDirect
Tetrahedron 64 (2008) 1798–1807
Tetrahedron
www.elsevier.com/locate/tet

Alkali metal complexation properties of resorcinarene bis-crown ethers: effect of the crown ether functionality and preorganization on complexation

Kirsi Salorinne, Maija Nissinen*

Department of Chemistry, Nanoscience Center, University of Jyväskylä, PO Box 35, 40014 JYU, Finland

Received 23 August 2007; received in revised form 13 November 2007; accepted 29 November 2007
Available online 4 December 2007

Abstract

The synthesis and characterization of tetramethoxy resorcinarene tribenzo-bis-crown ethers, ***m*-** and ***p*-TBBC6**, are described. The effect of the added aromatic functionality in the crown ether bridge on the alkali metal complexation properties was investigated and compared to the properties of tetramethoxy resorcinarene bis-crown-5 (**BC5**) by means of ^{1}H NMR spectroscopy and X-ray crystallography. It was found that **BC5** and ***m*-TBBC6** were capable of binding alkali metal cations (K^+, Rb^+, and Cs^+), with the highest affinity toward Cs^+ cation, while no binding was observed in the case of ***p*-TBBC6**, which confirms the significance of the complementarity and preorganization for complexation affinity.

Keywords: Calixcrown; Alkali metal cations; Complexation studies; Conformational analysis

1. Introduction

The complexation of alkali metal cations and their noncovalent interactions with host molecules have engaged a lot of interest due to their importance in chemical and biological systems.[1] A special point of interest has been cation–π interactions,[1,2] which have been intensively studied especially in gas phase[3] and with the help of theoretical studies,[4] and also to some extent in crystalline state.[2,5] In order to investigate these interactions that prevail in the host–guest system, the design of complementary host–guest pairs is an important aspect in developing new macrocyclic and macrobicyclic ligands that are able to selectively complex a specific guest. The criteria set for the host in molecular recognition include complementarity in respect to size and charge, sufficient flexibility, and preorganization, as well as induced fit upon guest binding.[6]

Calixcrowns[7] are a widely studied family of compounds, in which the properties arising from the rigid and preorganized calixarene skeleton are united with the abilities of crown ether to selectively bind cations.[8] Inspired by this union, we sought to take it one step further and replaced the calixarene framework with tetramethoxy resorcinarene,[9] thus, creating an assembly with two crown ether bridges on the open end of the resorcinarene cavity capable of hosting two cations in the formed crown pockets (Scheme 1).[10] Our earlier studies showed that tetramethoxy resorcinarene bis-crown-5 (**BC5**) was able to bind Cs^+ cation, but had affinity toward K^+ and Rb^+ cations as well.[10]

As has been demonstrated earlier,[11] the selectivity in cation binding is determined by the number of oxygen atoms in the crown ether moiety. In addition, alkali metal cations are known to form cation–π interactions with their host molecule.[2,12] An example of utilizing both these features is a cesium receptor by Bryan et al.,[13] which was based on the crown ether framework and *m*-xylene as a donor group. Also, Vicens et al.[14] have shown that introducing aromatic spacers in the crown bridges favored the complexation of cesium cation over the other alkali metal cations.

With this in mind, our scope was to improve the design of the resorcinarene bis-crown ethers by introducing aromatic functionality in the crown ether bridge with the idea that

* Corresponding author. Tel.: +358 14 260 4242; fax: +358 14 260 4756.
E-mail address: maija.nissinen@jyu.fi (M. Nissinen).

0040-4020/$ - see front matter © 2007 Elsevier Ltd. All rights reserved.
doi:10.1016/j.tet.2007.11.103

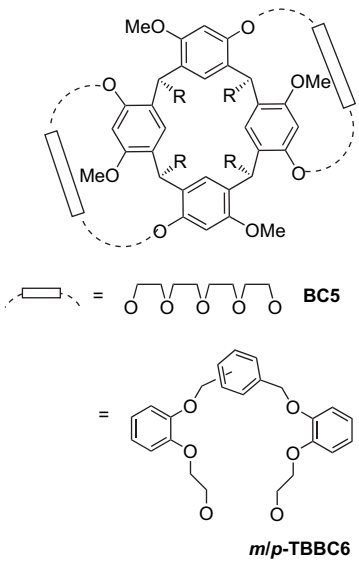

Scheme 1. Schematic presentation of tetramethoxy resorcinarene bis-crown ethers **BC5** and ***m*/*p*-TBBC6** ($R=C_2H_5$).

selectivity toward Cs^+ cation would be enhanced over K^+ and Rb^+ cations. We report here the synthesis and characterization of tetramethoxy resorcinarene bis-crowns *m*- and *p*-tribenzo-bis-crown-6 (***m*- and *p*-TBBC6**), both of which have three benzene rings in the crown bridge, yet differ from one another by the position of the central aromatic ring (Scheme 1). In addition, alkali metal binding abilities of **BC5** and ***m*/*p*-TBBC6** were investigated and compared by means of ^1H NMR and UV–vis spectroscopies, and X-ray crystallography.

2. Results and discussion

2.1. Synthesis and characterization

The aromatic crown bridges (Scheme 2) were obtained by the reaction of *m*/*p*-bis(bromomethyl)benzene with 2 equiv of 2-(2-hydroxyethoxy)phenol in the presence of K_2CO_3 in acetone affording **1a/b** in 65 and 94% yield, respectively. Subsequent reaction of **1a/b** with *p*-toluenesulfonyl chloride in the presence of triethylamine in dichloromethane gave ditosylates **2a/b** in 58 and 81% yield, respectively. Resorcinarene bis-crowns ***m*- and *p*-TBBC6** were finally accomplished by the reaction of the appropriate ditosylate **2** with tetramethoxy resorcinarene[9] in acetonitrile or DMF using excess of Cs_2CO_3 as the base with yields of 18 and 42%, respectively.

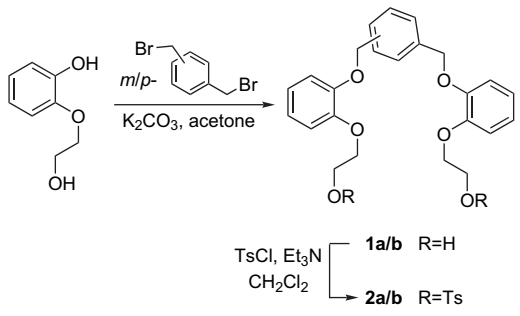

Scheme 2. Synthesis of aromatic crown bridges of ***m*/*p*-TBBC6**.

The structures of ***m*/*p*-TBBC6** and their precursors were characterized by means of NMR (^1H, ^{13}C, and 2D NMR) and mass (ESI^+) spectroscopies, X-ray crystallography, and elemental analysis, which all confirmed the success of the reactions.

2.2. Conformational studies by NMR and X-ray crystallography

As the crown bridges are formed over the adjacent aromatic rings of the resorcinarene skeleton, there no longer exist hydrogen bonds on the upper rim of the resorcinarene bowl and the symmetry is reduced to adopt a boat conformation. This can be seen in the proton NMR spectra by doubling of the resonances arising from the resorcinarene core. Since the conformation is locked by the crown bridges, and there cannot be any boat-to-boat interconversions, the environment of the upright aromatic and methoxy protons differs from the respective protons in the horizontal plane, and the resonances of these protons in these two environments become distinctly different giving rise to two sets of resonances (Fig. 1).

Although ***m*- and *p*-TBBC6** differ only by the position of the central benzene ring in the crown bridges, their conformations are very different from one another. The $-CH_2-$ resonances belonging to the crown ether bridge, which are seen in the 3–5 ppm area of the proton NMR spectra, are more resolved in the case of ***p*-TBBC6** than in the spectra of ***m*-TBBC6** indicating that the crown ether bridge of ***p*-TBBC6** is more rigid in structure and has less molecular motion. This was also evidenced by variable temperature NMR experiment. An increase of temperature from room temperature to 60 °C resulted in only slight changes in the chemical shifts of the protons in the crown bridge of ***m*-TBBC6**, whereas the changes in the corresponding resonances of ***p*-TBBC6** were significantly greater. The opposite was observed when the temperature was lowered from room temperature to −50 °C as the resolution of the spectra of ***p*-TBBC6** occurred already at −10 °C, while with ***m*-TBBC6** the spectra did not resolve completely until −50 °C. From this it can be concluded that there is more molecular motion within ***m*-TBBC6** due to the more flexible crown bridges (Fig. 2).

Single crystals suitable for crystal structural determination were obtained by slow evaporation from acetonitrile and acetonitrile–chloroform (structures A and B for ***m*-TBBC6**, respectively), and chloroform–dibenzylamine (***p*-TBBC6**) solutions. The obtained crystal structures confirmed the boat conformation of the resorcinarene bis-crowns ***m*-** and ***p*-TBBC6**, and, more importantly, they revealed the very different positions of the crown ether moieties in respect to the resorcinarene cavity for these two host molecules. In ***m*-TBBC6** the crown bridge unfolds over the aromatic ring of the resorcinarene skeleton in the horizontal plane creating a crown pocket with an aromatic ring as the base (Fig. 3). On the contrary, in ***p*-TBBC6** the crown bridges are formed by encircling the upright aromatic rings from outside and creating two loops rather than pockets as in ***m*-TBBC6** (Fig. 4).

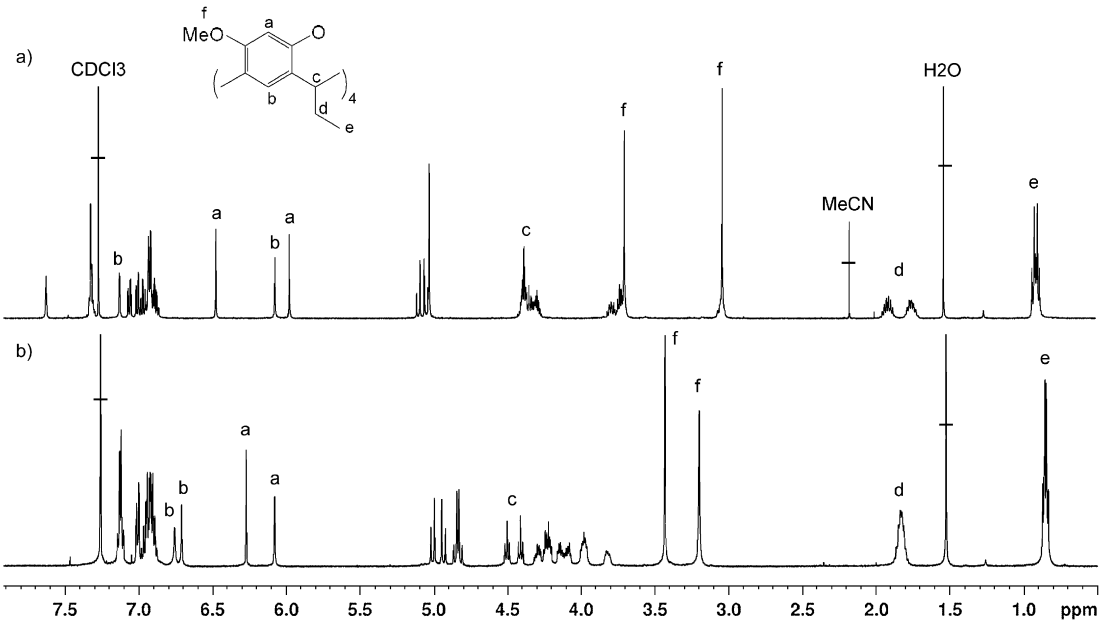

Figure 1. ^{1}H NMR spectra of (a) ***m*-TBBC6** and (b) ***p*-TBBC6** in $CDCl_3$. The chemical shifts of the resorcinarene core are indicated with letters showing the two sets of resonances for the aromatic and methoxy protons.

The difference in flexibility between ***m*-** and ***p*-TBBC6** observed in the ^{1}H NMR spectroscopic experiments was also evident in the obtained crystal structures. ***m*-TBBC6** crystallized in two distinct conformations, in which the crown bridges were either bent over the resorcinarene cavity (structure A) or stretched out sideways away from the cavity (structure B, Fig. 3). In structure A, the upright aromatic rings of the resorcinarene core are inclined outward opening up the cavity with an angle of 28.4° between the opposite aromatic rings, whereas in structure B the aromatic rings were slightly bent toward one another with an angle of −7.2° (the distances between the centroids of the opposite aromatic rings are 5.6 and 4.8 Å in the structures A and B, respectively). Three acetonitrile molecules occupy the resorcinarene cavity in structure A, while in structure B the cavity is too confined to include any solvent molecules, but the solvents are situated above the host via weak interactions to host. In both of these structures the molecules are packed in the crystal lattice in a manner, in which the crown bridges of the neighboring molecules are interlocked and held together through multiple CH−π and π−π interactions having distances in the range of 2.8−3.4 Å (Fig. 5).

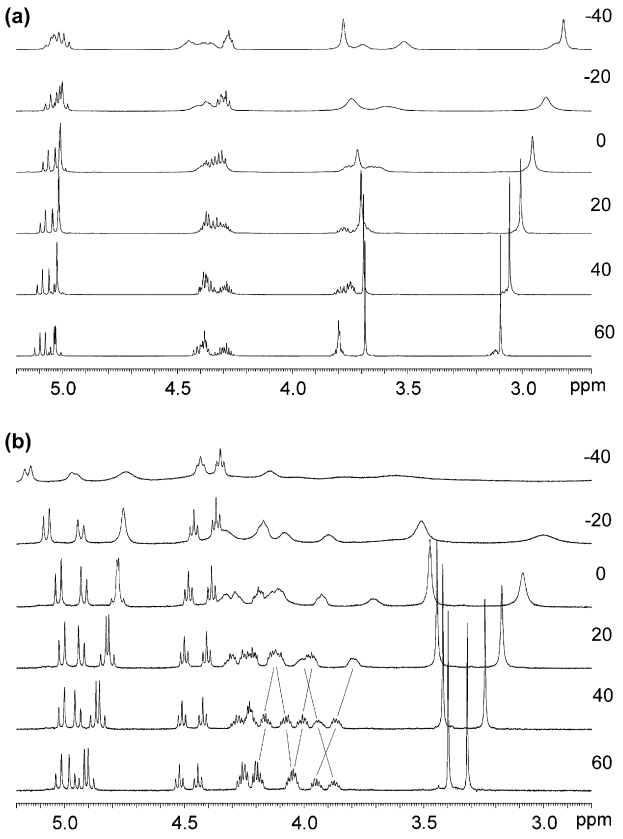

Figure 2. ^{1}H NMR variable temperature experiment of (a) ***m*-TBBC6** and (b) ***p*-TBBC6** in $CDCl_3$ showing the changes in the 3−5 ppm area of the spectra at a temperature range of 60 to −40 °C.

In the crystal structure of ***p*-TBBC6**, on the other hand, the crown loops had flapped out on the side of the molecule (structure C, Fig. 4). The resorcinarene cavity opened up, having an angle of 35.0° between the opposite upright aromatic rings (the distance between the centroids of the opposite aromatic rings is 5.7 Å) and is, therefore, able to include a part of the neighboring molecule inside the cavity forming a sandwich-like structure with the cavities of the two molecules facing one another while leaving no room for solvent inclusion. Again, multiple CH−π and π−π interactions between the neighboring molecules prevail in the crystal packing with distances in the range of 2.8−3.2 Å.

2.3. Complexation studies

The binding abilities of **BC5** and ***m*/*p*-TBBC6** toward alkali metal cations (K^+, Rb^+, and Cs^+) were investigated by

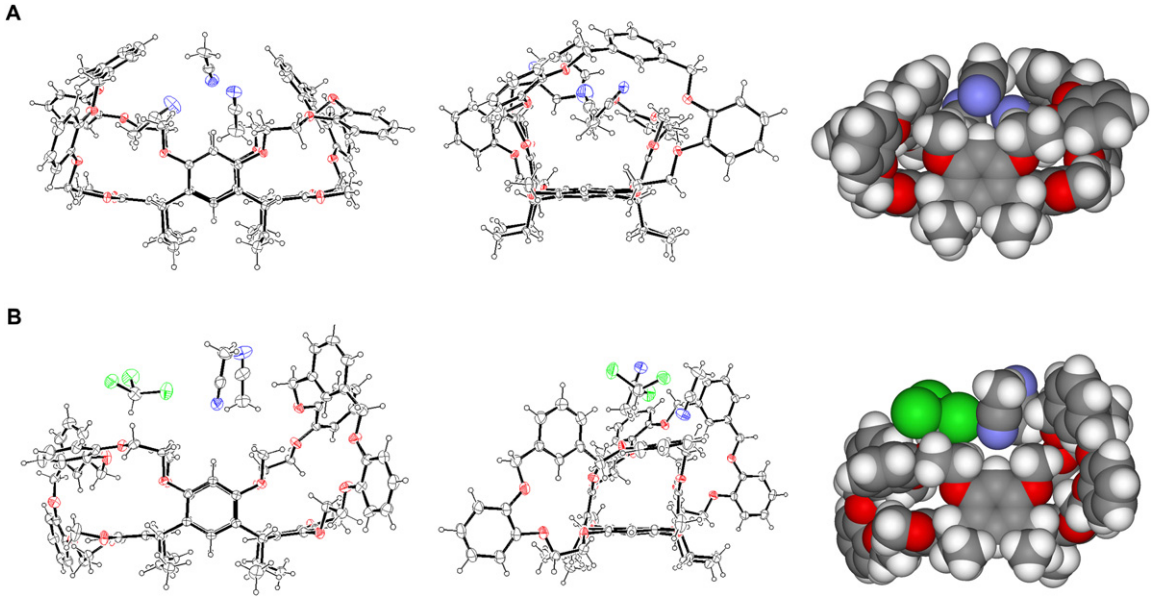

Figure 3. Ortep plot (front and side views) and VDW presentation (side view) showing the different conformations of the structures A (top) and B (bottom) of ***m*-TBBC6**. Solvent molecules in the crystal lattice are omitted for clarity.

means of ^{1}H NMR titration and picrate extraction experiments. The titration experiments of **BC5** were carried out in acetone-d_6, whereas with ***m*-** and ***p*-TBBC6**, acetonitrile-d_3 or 1:3 mixture of $CDCl_3$–CD_3CN was used due to solubility problems. Complexation-induced chemical shifts, particularly of the crown ether resonances in the respective ^{1}H NMR spectra, were observed after the addition of $RbPF_6$ and $CsPF_6$ salts in the solutions of **BC5** and ***m*-TBBC6**. With **BC5**, the addition of KPF_6 also induced changes in the crown ether region of the spectrum, but no changes were observed with any of the alkali metal salts in the presence of ***p*-TBBC6** as the host. The lack of complex formation in the case of ***p*-TBBC6** is explained by the rigid structure and unfavorable conformation of the host established in the conformational studies.

As a result of the inclusion of the cation in the crown pocket, the fairly flexible crown bridge should adopt a more

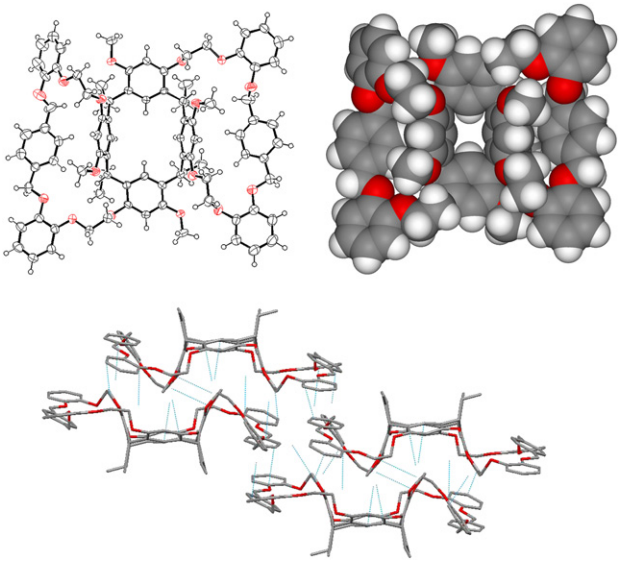

Figure 4. Top: Ortep plot and VDW presentation of ***p*-TBBC6** (top views). Solvent molecules are omitted for clarity. Bottom: crystal packing of ***p*-TBBC6** (side view). Blue lines indicate the CH–π and π–π interactions between the neighboring molecules. Hydrogens and solvent molecules in the crystal lattice are omitted for clarity.

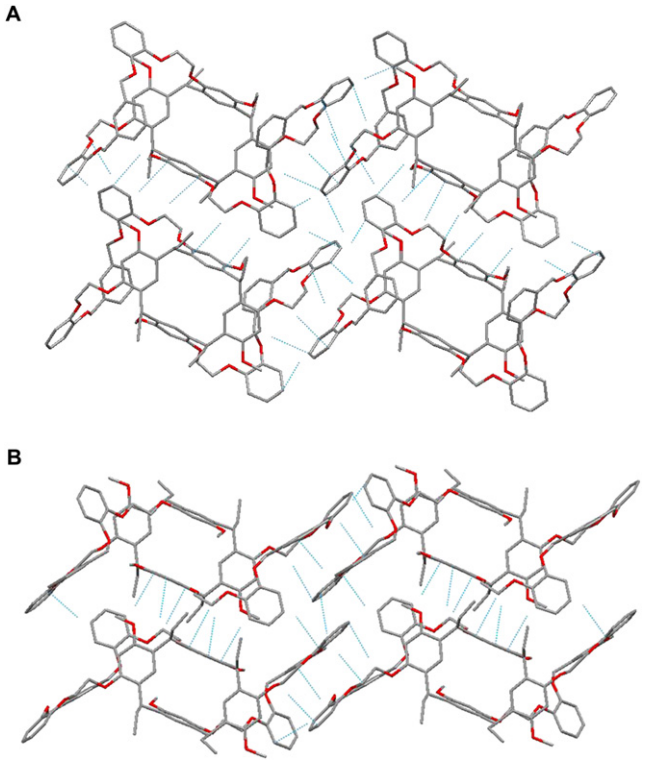

Figure 5. Crystal packing of the structures A (top) and B (bottom) of ***m*-TBBC6** (top views). Blue lines indicate the CH–π and π–π interactions between the neighboring molecules. Hydrogens and solvent molecules are omitted for clarity.

rigid form and simplify the spectrum in the crown ether region. In fact, upon increasing the amount of the added salt, resolution of the crown ether resonances of the respective host was observed, which was similar in pattern with the different cations investigated. In the case of **BC5**, the addition of $CsPF_6$ induced changes in the spectrum already with 1:1 molar ratio of the cation, whereas with KPF_6 and $RbPF_6$ the same changes required excess amount of the added salt. The inclusion of Cs^+ cation in the cavity of **BC5** also caused significant changes in the chemical shifts of the aromatic protons in the resorcinarene skeleton, which were not observed to the same extent with the other cations. This suggests that the inclusion of the guest in the crown pocket also causes changes in the conformation of the resorcinarene core and in the case of Cs^+ cation, there seems to be substantial interaction with the aromatic walls of the cavity through cation–π interaction.[12] A similar effect was observed with ***m*-TBBC6** as the host. The addition of $CsPF_6$ resulted in changes in the chemical shifts and resolution of the resonances of the $-CH_2-$ and aromatic protons in the crown bridge as well as changes in the chemical shifts of the aromatic protons in the resorcinarene core (Fig. 6). With the addition of $RbPF_6$ the changes in the spectrum were smaller, requiring excess amounts of the salt and contributed only to the changes in the chemical shifts but not to resolution of the spectra.

Since there are two crown ether pockets in both host molecules, which can each accommodate one guest species, we expected 1:2 host-to-guest complex formation. The stoichiometry was determined by modified Job analysis of continuous variations.[15] Interestingly, it was observed in the case of **BC5** that when the intrinsic water content of the NMR solvent was less than 0.3 molar ratio relative to host, Job plot analysis gave a maximum corresponding to 1:2 complex formation. Whereas with 2 molar ratio of water in relation to host, the stoichiometry of the complex species present was observed to be 1:1. This indicates that water plays a crucial role in complex formation, whether it is due to solvation effects of the alkali metal cations[16] or competitive binding in the crown pocket of the host molecule.[17] The stoichiometry of ***m*-TBBC6** could not be determined due to solubility problems at higher concentrations of the host molecule, although it was assumed to have a similar binding model to **BC5** based on the similarity in structure.

Table 1
Binding constants (M^{-1}) of 1:1 complexes of **BC5** and ***m*-TBBC6** with MPF_6[19]

Host	KPF_6	$RbPF_6$	$CsPF_6$
BC5	1.7[b]	4.5[b]	56.5[a]
***m*-TBBC6**	—	2.2[a]	35.3[a]

[a] Errors <20%.
[b] Error 30–40%.

Since the water content of the samples in the titration experiments exceeded 1 molar ratio relative to host, EQNMR analysis[18] of the titration data was fitted to a 1:1 binding model (Table 1). The stability constant data show that both **BC5** and ***m*-TBBC6** have one order of a magnitude higher affinity for Cs^+ cation than for Rb^+ and K^+ cations. Also, **BC5** has a slightly stronger binding compared to ***m*-TBBC6**. This could be explained partly by preorganization of the crown bridge.[13] The more extended crown bridge of ***m*-TBBC6** has more freedom to orient in different conformations, which may hinder the cation binding as more energy is needed to be applied in order to reach the suitable conformation. In **BC5** the crown pocket is almost circular and has an average cavity diameter of 6.05–6.31 Å.[10] With ***m*-TBBC6** the average cavity diameters are 5.58–5.68 Å (structure A) and 6.29–6.37 Å (structure B), but the cavity of the crown pocket is elliptical in shape and the longest cavity diameters measure up to 6.75–7.21 Å (structure A) and 9.46–10.10 Å (structure B) depending on the conformation. Although ***m*-TBBC6** has more aromatic functionality in the crown bridge, and should therefore increase the favorable cesium–π interactions[12] in addition to the aromatic cavity of the resorcinarene core, it seems that the crown pocket of **BC5** may provide a better complementarity in respect to shape and size.

Alkali metal picrate extraction experiments from water into chloroform confirmed the binding properties of the different hosts with K^+, Rb^+, and Cs^+ picrates. With ***p*-TBBC6** as the host, no alkali metal cations were extracted into the organic layer as was expected from the ^1H NMR titration experiments. In the case of ***m*-TBBC6** only Cs^+ was extracted,

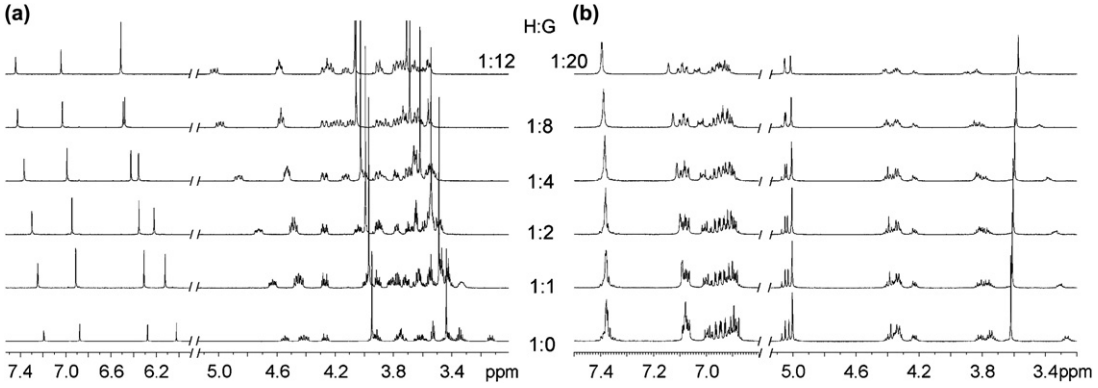

Figure 6. ^1H NMR titration spectra of (a) **BC5** with $CsPF_6$ in acetone-d_6 and (b) ***m*-TBBC6** with $CsPF_6$ in $CDCl_3$–CD_3CN (1:3) showing the changes in the aromatic and crown ether area of the spectra with different host–guest ratios.

Table 2
Alkali metal picrate extraction experiments[a]

Host	K^+	Rb^+	Cs^+
BC5	1.3	4.8	6.7
***m*-TBBC6**	0	0	3.4
***p*-TBBC6**	0	0	0

[a] Percentage (%) of picrate extracted from water into chloroform. Standard deviation of <0.01.

whereas **BC5** showed extraction ability toward all of the alkali metal cations studied (Table 2). Similar trends in selectivity were observed as in the ^{1}H NMR titration experiments with the highest affinity toward Cs^+ cation.

2.4. Crystal structures of the alkali metal complexes of *BC5*

The reaction of **BC5** with $RbPF_6$ and $CsPF_6$ in acetone afforded single crystals of the complexes of **BC5**·2$RbPF_6$·2Me_2CO and **BC5**·2$CsPF_6$.[20] Both of these structures show inclusion of one cation in each of the crown pocket of **BC5** confirming 1:2 (host–guest) complex formation. The structures are almost isomorphous with the exception that the structure of **BC5** with $RbPF_6$ contains solvent molecules in the crystal lattice. **BC5** also formed a complex with KPF_6, **BC5**·2KPF_6·2MeCN·H_2O, which has been reported earlier.[10] No crystals of the complexes of ***m*-TBBC6** with $RbPF_6$ or $CsPF_6$ have so far been obtained, which also supports the results of weaker complexation affinity.

In both of the structures of **BC5** the cations are bound tightly in the resorcinarene cavity and the angle between the upright aromatic rings of the resorcinarene core is 17.8° and 22.8° for the **BC5**·$RbPF_6$ and **BC5**·$CsPF_6$ complexes, respectively. The same angle in the conformation of **BC5** without the salts[10] is 31.6°, which clearly shows the participation of the resorcinarene core in complex formation by narrowing the cavity. Both cations coordinate to four crown ether oxygens in the crown bridge, to one methoxy oxygen, and to the aromatic ring in the crown pocket (Table 3). Additionally, the cations are coordinated to one of the PF_6^- counter anions that lies

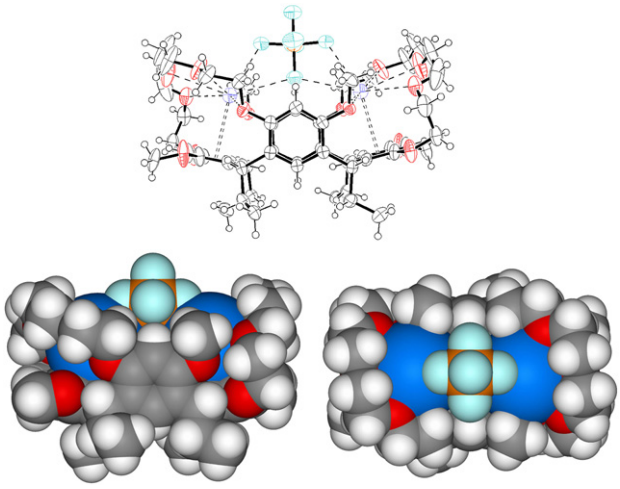

Figure 7. Ortep plot (top and front views) and VDW presentations (bottom, front, and top views) of the **BC5**·$CsPF_6$ complex. Noncoordinating solvent molecules are omitted for clarity.

inside the cavity between the two cations, while the other one contributes to the crystal packing outside the host molecule (Fig. 7). A similar binding of K^+ cation in the crown pocket was also observed in the complex of **BC5**·KPF_6 with the exception that the PF_6^- counter anion was situated between two K^+ cations of neighboring **BC5**·KPF_6 complexes inside the formed capsule.[10] The cation–π interaction in the structures of **BC5**·$RbPF_6$ and **BC5**·$CsPF_6$ follows the η^6-coordination mode, which has been shown to be ideal in theoretical studies,[1b,12] whereas in the structure of **BC5**·KPF_6, the K^+ cation is slightly off-centered from the aromatic ring toward the crown ether bridge.[10] These differences in the structures of the complexes of **BC5** with KPF_6 and $RbPF_6$ or $CsPF_6$ demonstrate that the crown pocket of **BC5** is adaptable enough to accommodate guest species differing in size.

Both of the structures are packed in the crystal lattice in a similar fashion, in which the molecules are lined up on top of one another forming vertical piles. These stacks then pack to form layers, in which the neighboring piles are facing in

Table 3
Selected bond lengths (Å) of the alkali metal complexes of **BC5**

BC5·KPF_6x		**BC5**·$RbPF_6$		**BC5**·$CsPF_6$	
K2···O4	3.113(3)	Rb···O6	3.080(5)	Cs···O6	3.184(3)
K2···O43	2.805(3)	Rb···O43A	2.965(5)	Cs···O43	3.011(4)
K2···O46	2.926(3)	Rb···O46A	3.00(2)	Cs···O46	3.186(4)
K2···O49	2.799(3)	Rb···O49	3.268(6)	Cs···O49A	3.269(7)
K1···O18	2.817(3)	[b]	[b]	[b]	[b]
K1···O54	3.872(3)	[b]	[b]	[b]	[b]
K1···O57	2.860(3)	[b]	[b]	[b]	[b]
K1···O60	2.853(3)	[b]	[b]	[b]	[b]
K2···O20	3.020(3)	Rb···O4	3.099(4)	Cs···O4	3.177(3)
K2···Ct1[a]	3.198(2)	Rb···Ct1[a]	3.151(3)	Cs···Ct1[a]	3.202(2)
K1···Ct2[a]	3.149(2)	[b]	[b]	[b]	[b]
K2···F11B	2.838(3)	Rb···F12	3.015(7)	Cs···F22A	2.973(7)
K1···F13A	2.728(3)	Rb···F14A	3.482(4)	Cs···F24	3.303(1)
K1···F16A	2.785(3)	—	—	—	—

[a] Ct1=Ct_{C8-C13} and Ct2=$Ct_{C22-C27}$.
[b] The coordination of both cations in the crown pocket is identical due to symmetry. See crystallographic numbering in Supplementary data.

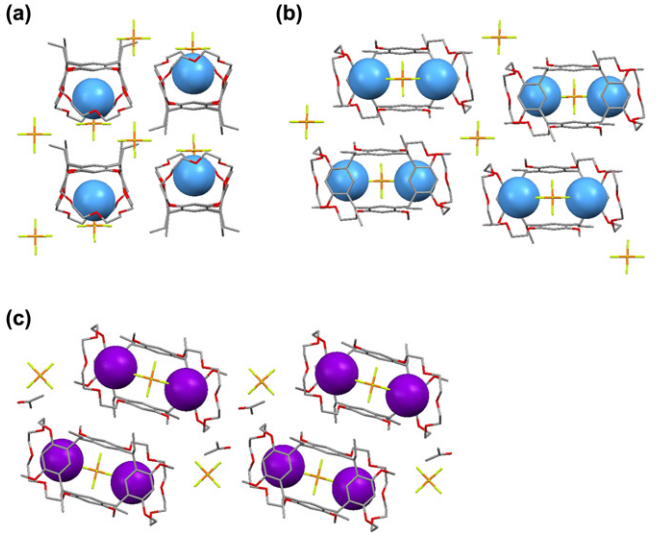

Figure 8. Crystal packing of the complexes of **BC5** with $CsPF_6$ and $RbPF_6$: (a) sideview of **BC5**·$CsPF_6$ (same for the complex of **BC5**·$RbPF_6$), (b) top view of **BC5**·$CsPF_6$, and (c) top view of **BC5**·$RbPF_6$. Hydrogens are omitted for clarity.

different directions (Fig. 8a). The difference between the almost isomorphous structures of **BC5**·$CsPF_6$ and **BC5**·$RbPF_6$ is that with **BC5**·$RbPF_6$ there are molecules of solvent acetone packed in the crystal lattice, which make the layers diagonal to one another, while with **BC5**·$CsPF_6$ the layers are in straight line (Fig. 8b and c).

3. Conclusions

In conclusion, tetramethoxy resorcinarene tribenzo-bis-crown ethers ***m*-** and ***p*-TBBC6** were prepared and their binding properties with alkali metal cations were studied and compared together with the earlier prepared **BC5**. The conformational studies of ***m*-** and ***p*-TBBC6** showed that preorganization provided by the resorcinarene skeleton, yet sufficient flexibility in the binding site, is an important feature of the host in complex formation. Of these three hosts, **BC5** and ***m*-TBBC6** showed affinity in binding alkali metal cations (K^+, Rb^+, and Cs^+), while no binding was observed with ***p*-TBBC6**. The binding in ***m*-TBBC6** was observed to be more selective compared to **BC5** since ***m*-TBBC6** bound Cs^+ cation almost exclusively, whereas **BC5** was able to bind K^+ and Rb^+ cations as well. However, the binding affinity of **BC5** toward cesium was almost two times higher than in the case of ***m*-TBBC6**. This indicates that the crown pocket of **BC5** is more preorganized in respect to shape and size and offers a better fit to Cs^+ cation, even without the added aromatic functionality of ***m*-** and ***p*-TBBC6**. This again shows the importance of host complementarity in the design of ligands in order to obtain selectivity and affinity in guest binding. In our future research, we plan to investigate the family of resorcinarene bis-crown ethers further by introducing different functionalities at the crown bridges and study the effects on complex formation.

4. Experimental

4.1. General

NMR spectra were recorded on Bruker Avance DRX (500 MHz for ^1H and 126 MHz for ^{13}C) spectrometer. ESI mass spectra were measured with Micromass LCT ESI-TOF instrument. Melting points were obtained with Stuart Scientific SMP3 melting point apparatus and are uncorrected. Elemental analyses were performed on Vario EL III apparatus. UV–vis spectra was recorded with Varian Cary 100 Conc UV–visible spectrophotometer.

4.2. Materials

All materials were commercial and used as such unless otherwise mentioned. Tetramethoxy resorcinarene was prepared according to the literature procedure[9] and **BC5** as previously described.[10] $RbPF_6$ and $CsPF_6$ were prepared by adding a saturated aqueous solution of NH_4PF_6 to an aqueous solution of RbCl or CsCl, respectively, followed by filtration and drying in vacuum.[21] DMF was distilled and stored over Linde type 3 Å molecular sieves prior use. Dichloromethane, acetonitrile, and acetone were distilled over $CaCl_2$ and stored over Linde type 3 Å molecular sieves prior use. K_2CO_3 and Cs_2CO_3 were dried in the oven at 120 °C and stored in a desiccator.

4.3. Synthesis

4.3.1. *m*/*p*-Bis-(2-ethoxyphenyloxy)xylene, ***1a*/*b***

A mixture of dibromo-*m*/*p*-xylene (4.3 g, 1.6 mmol), 2-(2-hydroxyethoxy)phenol (5.0 g, 3.3 mmol), K_2CO_3 (4.5 g, 3.3 mmol), and 18-crown-6 (2 mol %) was suspended in dry acetone (50 mL) under nitrogen atmosphere with stirring. The reaction mixture was refluxed overnight. After cooling to room temperature, the reaction mixture was filtered by suction and evaporated to dryness under vacuum. The resulting white solid was dissolved in dichloromethane and washed with water, dried over $MgSO_4$, and evaporated to dryness under vacuum. Compound **1a**: recrystallization from methanol afforded 4.2 g (65%) of white crystalline solid. ^1H NMR: ($CDCl_3$) δ 7.67 (s, 1H), 7.40–7.38 (m, 3H), 6.99–6.92 (m, 8H), 5.11 (s, 4H), 4.09 (t, J=4.4 Hz, 4H), 3.86 (t, J=3.3 Hz, 4H), 2.20 (br s, 2H) ppm. ^{13}C NMR: ($CDCl_3$) δ 149.0, 148.9, 137.5, 128.8, 127.4, 127.0, 122.0, 121.9, 115.2, 115.0, 71.6, 71.5, 61.2 ppm. MS (ESI-TOF): *m*/*z* 433.09 $[M+Na]^+$. Anal. Calcd for $C_{24}H_{26}O_6$: C, 70.23; H, 6.39. Found C, 69.94; H, 6.21. Mp 75–77 °C. Compound **1b**: recrystallization from hexane–methanol afforded 6.3 g (94%) of white solid. ^1H NMR: ($CDCl_3$) δ 7.45 (s, 4H), 6.99–6.94 (m, 8H), 5.11 (s, 4H), 4.11 (t, J=4.5 Hz, 4H), 3.86 (t, J=4.5 Hz, 4H) ppm. ^{13}C NMR: ($CDCl_3$) δ 149.4, 148.9, 136.9, 127.8, 122.3, 121.9, 116.2, 115.1, 71.8, 71.3, 61.3 ppm. MS (ESI-TOF): *m*/*z* 433.13 $[M+Na]^+$. Anal. Calcd for $C_{24}H_{26}O_6 \cdot 0.25H_2O$: C, 69.47; H, 6.44. Found C, 69.23; H, 6.22. Mp 110–112 °C.

*4.3.2. Ditosylate of m/p-bis-(2-ethoxyphenyloxy)xylene, **2a**/**b***

A mixture of **1a/b** (1.0 g, 2.4 mmol) and *p*-toluenesulfonyl chloride (1.0 g, 5.4 mmol) was suspended in dry dichloromethane (30 mL) under nitrogen atmosphere with stirring. Triethylamine (1.3 mL, 9.6 mmol) in dichloromethane was added dropwise and the reaction mixture was stirred at room temperature for 2 days. The reaction mixture was neutralized by the addition of 2 M HCl solution. The organic layer was washed two times with water, dried over $MgSO_4$, and evaporated to dryness under vacuum. Compound **2a**: purification by column chromatography on silica ($CHCl_3$–acetone, 9:1) afforded 1.0 g (58%) of opaque viscous oil. ^{1}H NMR: ($CDCl_3$) δ 7.77 (m, 4H), 7.49 (s, 1H), 7.38 (d, J=1.3 Hz, 3H), 7.25 (m, 4H), 6.93–6.83 (m, 8H), 5.09 (s, 4H), 4.35 (m, 4H), 4.22 (m, 4H), 2.39 (s, 6H) ppm. ^{13}C NMR: ($CDCl_3$) δ 149.2, 148.3, 144.8, 137.6, 133.0, 129.8, 128.8, 127.9, 126.8, 126.1, 122.6, 121.7, 116.1, 115.5, 71.2, 68.3, 67.3, 21.6 ppm. MS (ESI-TOF): *m/z* 741.10 $[M+Na]^+$, 757.06 $[M+K]^+$. Compound **2b**: purification by column chromatography on silica (CH_2Cl_2–acetone, 9:1) afforded 1.4 g (81%) of white solid. ^{1}H NMR: ($CDCl_3$) δ 7.78 (m, 4H), 7.42 (s, 4H), 7.26 (m, 4H), 6.94–6.84 (m, 8H), 5.08 (s, 4H), 4.35 (m, 4H), 4.23 (m, 4H), 2.39 (s, 6H) ppm. ^{13}C NMR: ($CDCl_3$) δ 149.2, 148.4, 144.8, 136.8, 133.0, 129.8, 128.0, 127.5, 122.6, 121.8, 116.1, 115.5, 71.1, 68.3, 67.3, 21.6 ppm. MS (ESI-TOF): *m/z* 741.20 $[M+Na]^+$. Anal. Calcd for $C_{38}H_{38}O_{10}S_2\cdot 0.5H_2O$: C, 62.71; H, 5.40. Found C, 62.64; H, 5.19. Mp 112–113 °C.

*4.3.3. Tetramethoxy resorcinarene tribenzo-bis-crown-6, **m**/**p-TBBC6***

4.3.3.1. Method A. A mixture of tetramethoxy resorcinarene[9] (0.28 g, 0.43 mmol), Cs_2CO_3 (1.2 g, 3.8 mmol), and dibenzo-18-crown-6 (0.08 g, 0.22 mmol) in dry acetonitrile (70 mL) under nitrogen atmosphere was heated to reflux. The reaction mixture was allowed to stir for 30 min before the dropwise addition of ditosylate **2a** (0.61 g, 0.85 mmol) in acetonitrile and refluxed for 2 days. After cooling to room temperature the reaction mixture was filtered by suction and the solvent was removed under vacuum. Chloroform was added to the resulting residue and solid formed was filtered off by suction. ***m*-TBBC6**: purification by column chromatography on silica (chloroform–ethyl acetate 95:5) afforded 0.1 g (18%) of white crystalline solid. ^{1}H NMR: ($CDCl_3$) δ 7.61 (s, 2H), 7.31 (m, 6H), 7.12 (s, 2H), 7.06–6.86 (m, 16H), 6.46 (s, 2H), 6.06 (s, 2H), 5.97 (s, 2H), 5.06 (dd, J=11.4, 14.7 Hz, 4H), 5.02 (s, 4H), 4.39–4.28 (m, 12H), 3.81–3.72 (m, 6H), 3.70 (s, 6H), 3.03 (overlapping m and s, 8H), 1.90 (m, 4H), 1.75 (m, 4H), 0.90 (m, 12H) ppm. ^{13}C NMR: ($CDCl_3$) δ 156.1, 155.7, 155.2, 155.0, 149.7, 149.2, 149.0, 148.6, 137.9, 137.5, 129.7, 129.0, 128.4, 127.4, 127.3, 126.3, 125.5, 125.4, 122.2, 121.7, 121.6, 121.5, 116.1, 115.1, 115.0, 114.7, 71.8, 71.3, 69.4, 68.4, 68.0, 67.2, 55.6, 54.9, 37.1, 36.9, 27.9, 27.4, 12.6, 12.5 ppm. MS (ESI-TOF): *m/z* 1427.43 $[M+Na]^+$, 1443.43 $[M+K]^+$. Anal. Calcd for $C_{88}H_{92}O_{16}\cdot 0.75CHCl_3$: C, 71.29; H, 6.25. Found C, 71.19; H, 6.15. Mp 135–137 °C.

4.3.3.2. Method B. A mixture of tetramethoxy resorcinarene[9] (0.21 g, 0.31 mmol) and Cs_2CO_3 (0.72 g, 2.2 mmol) in dry DMF (25 mL) was stirred at 90 °C under nitrogen atmosphere for 20 min before the dropwise addition of ditosylate **2b** (0.44 g, 0.61 mmol) in dry DMF with vigorous stirring. The reaction mixture was stirred at 90 °C for 2 days. After cooling to room temperature the reaction mixture was filtered by suction through a pad of Hyflo Super® and solvent was removed under vacuum. The resulting residue was partitioned between water and dichloromethane, and acidified with 2 N HCl. The organic layer was separated, dried over $MgSO_4$, and evaporated to dryness under vacuum. ***p*-TBBC6**: purification by column chromatography on silica ($CHCl_3$–acetone, 9:1) afforded 0.18 g (42%) of white solid. ^{1}H NMR: ($CDCl_3$) δ 7.13 (q, J=8.3, 5.2 Hz, 8H), 7.02–6.88 (m, 16H), 6.76 (s, 2H), 6.71 (s, 2H), 6.27 (s, 2H), 6.08 (s, 2H), 4.96 (dd, J=12.0, 25.8 Hz, 4H), 4.84 (q, J=11.0, 6.7 Hz, 4H), 4.50 (t, J=7.6 Hz, 2H), 4.41 (t, J=7.6 Hz, 2H), 4.29 (m, 2H), 4.22 (m, 4H), 4.15–4.08 (m, 4H), 3.98 (m, 4H), 3.83 (m, 2H), 3.43 (s, 6H), 3.20 (s, 6H), 1.83 (m, 8H), 0.85 (m, 12H) ppm. ^{13}C NMR: ($CDCl_3$) δ 155.7, 155.5, 155.0, 149.9, 149.3, 149.2, 149.1, 136.8, 136.7, 127.8, 127.6, 127.3, 126.6, 126.5, 126.3, 125.5, 122.0, 121.8, 121.7, 121.5, 116.0, 115.5, 115.3, 114.5, 98.9, 98.8, 71.6, 71.0, 69.0, 68.7, 68.6, 68.3, 55.5, 55.1, 36.5, 36.4, 28.3, 28.1, 12.6, 12.5 ppm. MS (ESI-TOF): *m/z* 1428.59 $[M+Na]^+$. Anal. Calcd for $C_{88}H_{92}O_{16}\cdot 2H_2O$: C, 73.31; H, 6.71. Found C, 73.62; H, 6.44. Mp 133–135 °C.

4.4. ^{1}H NMR titration experiments

^{1}H NMR titrations were performed by subsequently adding increasing aliquots of the salt (KPF_6, $RbPF_6$, and $CsPF_6$) in deuterated solvent to solutions of the respective host (**BC5** in acetone-d_6, ***m*-TBBC6** in 1:3 mixture of $CDCl_3$–CD_3CN, and ***p*-TBBC6** in acetonitrile-d_3) and the spectra were recorded at 30 °C. The obtained titration data were analyzed by the computer program EQNMR.[18] Job plot samples were prepared with 0.5, 1, 1.5, 2, 3, and 4 equiv of the salt while keeping the sum of host and guest concentration equal.

4.5. Picrate extraction experiments

The alkali metal (Na^+, K^+, and Cs^+) picrate extraction experiments were performed by using 2.5 mM host solutions of **BC5** and ***m*-** and ***p*-TBBC6** in chloroform and 5 mM picrate solutions in deionized water according to the procedure described earlier.[10] The absorption of the extracted picrate was measured from the aqueous layer at 375 nm and compared against blank solution (no host in chloroform) of the appropriate picrate. The average of three samples is reported with standard deviation.

4.6. X-ray crystallography

Data were recorded on a Nonius Kappa CCD diffractometer with Apex II detector using graphite monochromatized Cu Kα [λ(Cu Kα)=1.54178 Å] radiation at a temperature of 173.0 K.

Table 4
Crystallographic details of ***m*-TBBC6** (structures A and B) and ***p*-TBBC6** (structure C) and the complexes of **BC5·RbPF$_6$** and **BC5·CsPF$_6$**

	***m*-TBBC6** (structure A)	***m*-TBBC6** (structure B)	***p*-TBBC6** (structure C)	**BC5**·$RbPF_6$	**BC5**·$CsPF_6$
Molecular formula	$C_{88}H_{92}O_{16}\cdot 7CH_3CN\cdot 0.25H_2O$	$C_{88}H_{92}O_{16}\cdot 3CH_3CN\cdot CHCl_3$	$C_{88}H_{92}O_{16}\cdot C_{14}H_{15}N$	$C_{56}H_{76}O_{14}\cdot 2RbPF_6\cdot 2(CH_3)_2CO$	$C_{56}H_{76}O_{14}\cdot 2CsPF_6$
Formula weight	1697.50	1648.15	1602.89	1550.20	1528.93
Crystal system	Monoclinic	Monoclinic	Monoclinic	Monoclinic	Monoclinic
Space group	$P2_1/n$ (no. 14)	$P2_1/c$ (no. 14)	$P2_1/n$ (no. 14)	$P2/c$ (no. 13)	$P2/c$ (no. 13)
a (Å)	21.3463(5)	17.4834(4)	16.2238(4)	20.3086(9)	18.2591(8)
b (Å)	22.1363(5)	20.0800(4)	30.5922(9)	10.0123(4)	9.8762(5)
c (Å)	22.0402(5)	25.1202(6)	18.1516(4)	19.7412(6)	19.8445(8)
β (°)	116.115(1)	102.913(1)	109.974(2)	118.180(2)	116.541(2)
Volume (Å^3)	9350.2(4)	8595.8(3)	8467.1(4)	3538.3(2)	3201.4(3)
Z	4	4	4	2	2
D_{calcd} (Mg m^{-3})	1.206	1.274	1.257	1.455	1.586
μ (mm^{-1})	0.659	1.522	0.674	3.043	10.188
GOF on F^2	1.026	1.017	1.019	1.070	1.077
Final R indices[a]	0.085/0.170	0.085/0.215	0.084/0.170	0.090/0.231	0.047/0.103

[a] ($I>2\sigma I$).

The data were processed with Denzo-SMN v0.97.638.[22] The structures were solved by direct methods (SHELXS-97[23]) and refinements based on F^2 were made by full-matrix least-squares techniques (SHELXL-97[24]). The hydrogen atoms were calculated to their idealized positions with isotropic temperature factors (1.2 or 1.5 times the C temperature factor) and refined as riding atoms, except for the amine hydrogen of dibenzoamine, which was located from the difference Fourier map (Table 4). Absorption correction[25] was made to all structures but used only in the final refinement of the structure of **BC5**·$2CsPF_6$ since it worsened the quality of all the other structures described. Crystallographic details of the structures are presented in Table 4. Crystallographic data (excluding structural factors) for the structures in this paper have been deposited with the Cambridge Crystallographic Data Center as supplementary publication nos. CCDC-658268, 658269, 658270, 658271, 658272, and 658273. Copies of the data can be obtained, free of charge, on application to CCDC, 12 Union Road, Cambridge CB2 1EZ, UK (fax: +44 (0) 1223 336033 or email: deposit@ccdc.cam.ac.uk).

Acknowledgements

We are grateful to Reijo Kauppinen (University of Jyväskylä) for his help with the NMR studies and the Academy of Finland (project 211240) for funding.

Supplementary data

Supplementary data associated with this article can be found in the online version, at doi:10.1016/j.tet.2007.11.103.

References and notes

1. (a) Rodgers, M. T.; Armentrout, P. B. *Acc. Chem. Res.* **2004**, *37*, 989–998; (b) Ma, J. C.; Dougherty, D. A. *Chem. Rev.* **1997**, *97*, 1303–1324; (c) Meyer, E. A.; Castellano, R. K.; Diederich, F. *Angew. Chem., Int. Ed.* **2003**, *42*, 1210–1250.
2. (a) Gokel, G. W.; De Wall, S. L.; Meadows, E. S. *Eur. J. Org. Chem.* **2000**, 2967–2978; (b) Gokel, G. W.; Barbour, L. J.; Ferdani, R.; Hu, J. *Acc. Chem. Res.* **2002**, *35*, 878–886.
3. See, for example: (a) Woodin, R. L.; Beauchamp, J. L. *J. Am. Chem. Soc.* **1978**, *100*, 501–508; (b) Dunbar, R. C.; Ryzhov, V. *J. Am. Chem. Soc.* **1999**, *121*, 2259–2268.
4. For review on the subject, see Ref. 1b. For more recent work see, for example: (a) Macias, A. T.; Norton, J. E.; Evanseck, J. D. *J. Am. Chem. Soc.* **2003**, *125*, 2351–2360; (b) Priyakumar, U. D.; Punnagai, M.; Mohan, G. P. K.; Sastry, G. N. *Tetrahedron* **2004**, *60*, 3037–3043.
5. (a) Cametti, M.; Nissinen, M.; Dalla Cort, A.; Mandolini, L.; Rissanen, K. *J. Am. Chem. Soc.* **2005**, *127*, 3831–3837; (b) Åhman, A.; Nissinen, M. *Chem. Commun.* **2006**, 1209–1211.
6. Schneider, H. J.; Anmar, K. M. Receptors for Organic Guest Molecules: General Principles. *Comprehensive Supramolecular Chemistry*; Atwood, J. L., Davies, J. E. D., Macnicol, D. D., Vögtle, F., Eds.; Pergamon: Oxford, UK, 1996; Vol. 2, pp 69–101.
7. (a) Ungaro, R. *Calixarenes in Action*; Mandolini, L., Ungaro, R., Eds.; Imperial College Press: London, UK, 2000; (b) Sharma, K. R.; Agrawal, Y. K. *Rev. Anal. Chem.* **2004**, *23*, 133–158; (c) Alfieri, C.; Dradi, E.; Pochini, A.; Ungaro, R.; Andreetti, G. D. *J. Chem. Soc., Chem. Commun.* **1983**, 1075–1077.
8. Steed, J. W. *Coord. Chem. Rev.* **2001**, *215*, 171–221.
9. McIldowie, M. J.; Mocerino, M.; Skelton, B. W.; White, A. H. *Org. Lett.* **2000**, *2*, 3869–3871.
10. Salorinne, K.; Nissinen, M. *Org. Lett.* **2006**, *8*, 5473–5476.
11. (a) Ghidini, E.; Ugozzoli, F.; Ungaro, R.; Harkema, S.; El-Fadi, A. A.; Reinhoudt, D. N. *J. Am. Chem. Soc.* **1990**, *112*, 6979–6985; (b) Stephan, H.; Gloe, K.; Paulus, E. F.; Saadioui, M.; Böhmer, V. *Org. Lett.* **2000**, *2*, 839–841; (c) Casnati, A.; Della Ca', N.; Sansone, F.; Ugozzoli, F.; Ungaro, R. *Tetrahedron* **2004**, *60*, 7869–7876.
12. Fukin, G. K.; Lindeman, S. V.; Kochi, J. K. *J. Am. Chem. Soc.* **2002**, *124*, 8329–8336.
13. Bryan, J. C.; Hay, B. P.; Sachleben, R. A.; Eagle, C. T.; Zhang, C.; Bonnesen, P. V. *J. Chem. Crystallogr.* **2003**, *33*, 349–355.
14. (a) Lamare, V.; Dozol, J. F.; Fuangswasdi, S.; Arnaud-Neu, F.; Thuéry, P.; Nierlich, M.; Asfari, Z.; Vicens, J. *J. Chem. Soc., Perkin Trans. 2* **1999**, 271–284; (b) Asfari, Z.; Lamare, V.; Dozol, J. F.; Vicens, J. *Tetrahedron Lett.* **1999**, *40*, 691–694.
15. Hirose, K. *J. Incl. Phenom. Macrocyclic Chem.* **2001**, *39*, 193–209.
16. Buschmann, H. J.; Wenz, G.; Schollmeyer, E.; Mutihac, L. *Inorg. Chem. Commun.* **2001**, *4*, 211–214.
17. Bauer, L. J.; Gutsche, C. D. *J. Am. Chem. Soc.* **1985**, *107*, 6063–6069.
18. Hynes, M. J. *J. Chem. Soc., Dalton Trans.* **1993**, 311–312.
19. The water content in relation to host in the titration experiments was 1–2 molar ratio with **BC5** and 2–4 molar ratio with ***m*-TBBC6** as the host.
20. Single crystals were obtained by slow evaporation from the NMR titration samples of **BC5** with RbPF6 and CsPF6 in acetone-d_6.
21. Fuchs, B.; Nelson, A.; Star, A.; Stoddart, J. F.; Vidal, S. *Angew. Chem., Int. Ed.* **2003**, *42*, 4220–4224.

22. Otwinowski, Z.; Minor, W. Processing of X-ray Diffraction Data Collected in Oscillation Mode. In *Macromolecular Crystallography, Part A*; Carter, C. W., Sweet, R. M., Eds.; Methods in Enzymology; Academic: New York, NY, 1997; Vol. 276, pp 307–326.
23. Sheldrick, G. M. *Acta Crystallogr., Sect. A* **1990**, *46*, 467–473.
24. Sheldrick, G. M. *A Program for Crystal Structure Refinement*; University of Göttingen: Göttingen, Germany, 1997.
25. Blessing, R. H. *Acta Crystallogr., Sect. A* **1995**, *51*, 33–38.